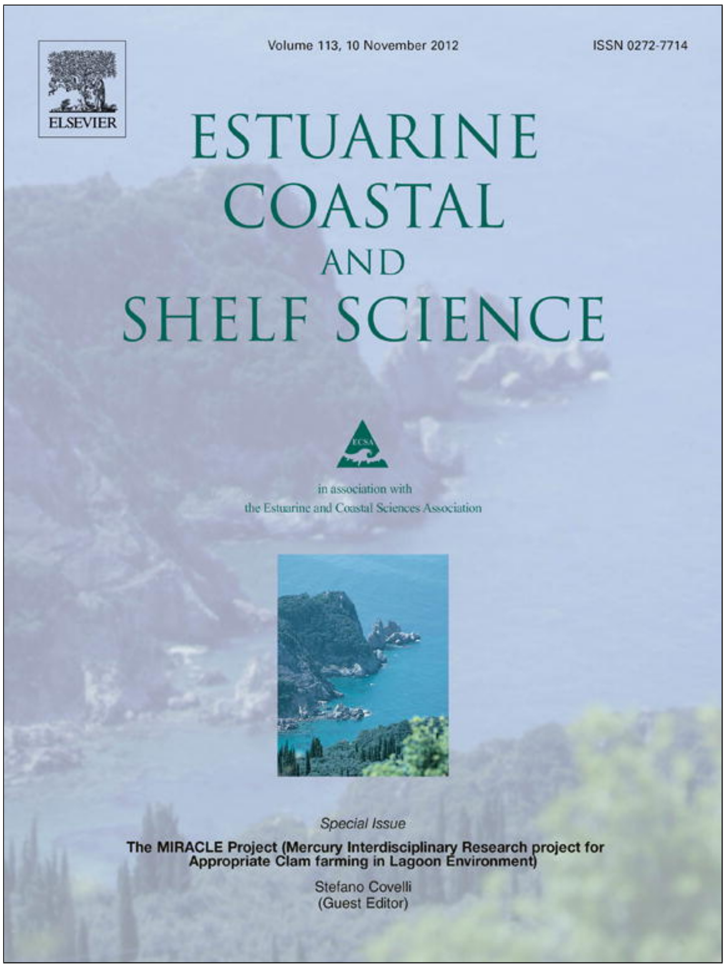

Volume 113, 10 November 2012 ISSN 0272-7714

ESTUARINE
COASTAL
AND
SHELF SCIENCE

in association with
the Estuarine and Coastal Sciences Association

Special Issue

The MIRACLE Project (Mercury Interdisciplinary Research project for Appropriate Clam farming in Lagoon Environment)

Stefano Covelli
(Guest Editor)

Estuarine, Coastal and Shelf Science 113 (2012) 7–19

Contents lists available at SciVerse ScienceDirect

Estuarine, Coastal and Shelf Science

journal homepage: www.elsevier.com/locate/ecss

Historical flux of mercury associated with mining and industrial sources in the Marano and Grado Lagoon (northern Adriatic Sea)

Stefano Covelli [a,*], Leonardo Langone [b], Alessandro Acquavita [a,c], Raffaella Piani [a], Andrea Emili [a]

[a] Dipartimento di Geoscienze, Università di Trieste, Via Weiss 2, 34128 Trieste, Italy
[b] CNR, Istituto di Scienze Marine (ISMAR), via Gobetti 101, 40129 Bologna, Italy
[c] Osservatorio Alto Adriatico, Agenzia Regionale per la Protezione dell'Ambiente del Friuli Venezia Giulia (ARPA-FVG), Via Cairoli 14, 33057 Palmanova, Italy

ARTICLE INFO

Article history:
Received 2 September 2011
Accepted 29 December 2011
Available online 4 January 2012

Keywords:
sediment
lagoon
mercury
contamination
geochronology
Adriatic Sea

ABSTRACT

The “MIRACLE” Project was established in order to assess the feasibility of clam farming and high levels of sediment mercury (Hg) contamination coexisting in the Marano and Grado Lagoon, Italy. This lagoon has been subjected to Hg input from both industrial waste (chlor-alkali plant) and long-term mining activity (Idrija mine, NW Slovenia). One of the subtasks of the “MIRACLE” Project was to determine the historical evolution of Hg accumulation in the lagoon's bottom sediments. Thirteen 1-m deep sediment cores were collected from the subtidal and intertidal zones, plus one in a saltmarsh, all of which were then analyzed for total Hg content and several physicochemical parameters. Sedimentation rate assessments were performed by measuring short-lived radionuclides (excess ^{210}Pb and ^{137}Cs). For most of the analyzed cores, natural background levels of Hg were observed at depths of 50–100 cm. In the eastern area, Hg contamination was found to be at its maximum level at the core top (up to 12 μg g^{-1}) as a consequence of the long-term mining activity. The vertical distribution of Hg was related to the influence of the single-point contamination sources, whereas the grain-size variability or organic matter content seemed not to affect it. In the western area, Hg content at the surface was found not to exceed 7 μg g^{-1} and contamination was recorded only in the first 20–30 cm. Geochronological measurements showed that the depositional flux of Hg was influenced by anthropogenic inputs after 1800, when mining activity was more intense. After 1950, Hg in the surface sediment, most remarkable in the central-western sector, seemed to also be affected by the discharge of the Aussa River, which delivers Hg from the chlor-alkali plant. In 1996, Hg mining at Idrija ceased, however the core profiles did not show any subsequent decreasing trend in terms of Hg flux, which implies the system retaining some “memory” of contamination. Thus, in the short term, a decrease in Hg inputs into the nearby Gulf of Trieste and the lagoon seems unlikely. A preliminary rounded-down gross estimate of total Hg “trapped” in the lagoon's sediments amounted to 251 t. Such a quantity, along with the complexity of the lagoon ecosystem, suggests that an *in toto* reclamation of the sediments at the lagoon scale is unfeasible, both economically and environmentally.

1. Introduction

Sediments in shallow coastal waters act as sinks for metals originating from both natural and anthropogenic sources. Fine-grained sediments in particular show an ability to accumulate metals from atmospheric deposition, from soil erosion, through transport from watersheds downstream to the aquatic environment, or directly from wastewater discharge. Among the metals found in coastal sediments, mercury (Hg) is of particular concern with regards to contamination due to both its high mobility (Fitzgerald et al., 2007) and the toxicity and bioavailability of its organic form (methylmercury) within the food web (Morel et al., 1998; Benoit et al., 2003). Many coastal ecosystems act as large reservoirs of Hg through their sediments (Covelli et al., 2001; Sager, 2002; Canário et al., 2005), and a number of controlling physical and chemical factors, such as grain-size, organic matter content (e.g. Benoit et al., 1998; Mason and Lawrence, 1999), co-precipitation with iron (Fe) and manganese (Mn) oxides (Gagnon et al., 1997; Muresan et al., 2007), and binding to sulphides (Gagnon et al., 1997; Fabbri et al., 2001), have been shown to affect the distribution of Hg within those sediments.

---

[*] Corresponding author. Present address: Dipartimento di Geoscienze, Università di Trieste, Via Weiss, 2, 34128 Trieste, Italy.
E-mail address: covelli@units.it (S. Covelli).

0272-7714/$ – see front matter © 2012 Elsevier Ltd. All rights reserved.
doi:10.1016/j.ecss.2011.12.038

The accumulation of Hg in coastal sediments can cause significant environmental problems (Mason and Lawrence, 1999; Trombini et al., 2003; Piani et al., 2005), since contaminated surface sediments can act as a potential secondary source of the metal to the aquatic ecosystem. The resuspension of sediments by natural (e.g. tidal fluxes, storm events) and anthropogenic (mainly channel dredging and clam harvesting) factors may cause the transport and dispersion of Hg from sediments, favouring the persistence of high levels of contamination in coastal lagoon environments (Bloom et al., 2004). The remobilization of Hg in dissolved form may occur through benthic fluxes from the sediment–water interface (Covelli et al., 1999, 2008; Point et al., 2007; Hammerschmidt and Fitzgerald, 2008), with possible further transport to estuarine and pelagic food webs (Lawson and Mason, 1998; Wiener et al., 2003). However, sediments may also represent reliable 'archives' for the history of Hg contamination, as well as other metals. They may even provide clues for tracing the sources of contamination in lagoons, estuaries, tidal flats and saltmarshes (e.g. Conaway et al., 2004; Kading et al., 2009; Ruiz-Fernández et al., 2009; Shi et al., 2010).

The Hg in the coastal environment reported upon in the present study (the Marano and Grado Lagoon, northern Adriatic Sea) is supplied by two anthropogenic sources. The first, an industrial complex that has been producing cellulose, chlor-alkali and artificial textile fibres since the 1940s, used to discharge its processing and seepage wastewaters into the Aussa-Corno River, the main watershed system locally, and consequently into the lagoon. Although direct discharge of Hg no longer takes place, the metal is still released from the contaminated industrial area into the river system, and its distribution and abundance in the lagoon is controlled by the salt wedge circulation system, which is influenced by the tide (Covelli et al., 2009). The second long-term Hg source in the area is the Isonzo River, which has been the largest contributor of this metal into the northern Adriatic Sea since the 16th century due to Hg mining in Idrija, western Slovenia (Horvat et al., 1999; Covelli et al., 2001). Despite the Idrija mine having been shut down in 1995, the contribution of Hg into the Gulf of Trieste remains considerable. Seasonal sampling at the Isonzo River mouth has demonstrated that dissolved and particulate Hg concentrations are still very high during low and normal river discharge throughout the year (Faganeli et al., 2003; Covelli et al., 2006a). During peak river discharge and river plume formation, fluvial suspended particulate matter represents the main input of Hg to the coastal waters of the Gulf of Trieste. Tidal fluxes act as a sort of natural "conveyor belt", transporting Hg bound to suspended particulates into the adjacent Marano and Grado Lagoon, where it eventually accumulates on the mudflats (Covelli et al., 2007). Piani et al. (2005), investigating Hg speciation in bottom sediments of the Marano and Grado Lagoon, demonstrated that cinnabar (HgS), mostly stable and insoluble, entering from the sea through tidal inlets, dominated the central sector of the lagoon. Conversely, organically-bound Hg, which can be transformed into bioavailable methylmercury, was found associated with fine-grained material accumulated near the Aussa-Corno River mouth.

This paper presents part of the results of the MIRACLE Project, an interdisciplinary study aimed to test the coexistence of clam farming in sediments where Hg content is recognized to be up to three orders of magnitude higher than the natural background, and the possible extension of the existing rearing activities to other areas of the Marano and Grado Lagoon. Since local fishing, the collection of clams and mussels, and edible fish cultivation are extensively practised, there is great concern about the risk posed by potentially harmful effects of Hg on the trophic chain (Brambati, 2001). The main aim of this work was to document the sedimentary records of Hg and, on the basis of ^{210}Pb and ^{137}Cs sedimentation rate assessments, to reconstruct the history of Hg contamination. By comparing Hg accumulation trends in different areas, we were able to distinguish between Hg inputs due to the 500 years of mining activity in Idrija from those resulting from local and more recent industrial sources. Finally, a cumulative metal inventory was also calculated in order to provide a preliminary estimation of anthropogenic Hg stored in the sediments of this lagoon environment.

2. Environmental setting

The Marano and Grado Lagoon is a shallow wetland system covering an area of 160 km^2 located along the northern Adriatic coast between the Tagliamento and Isonzo River deltas (Fig. 1). A long, 8-m deep canal, maintained by periodic dredging to be navigable for commercial shipping, separates the Marano Lagoon (western part) from the Grado Lagoon (eastern part). The lagoonal waters are affected by semi-diurnal tidal fluxes (mean and spring tidal range of 65 and 105 cm, respectively), and show salinity values ranging from 2 to 7 in the areas close to the river mouths, to 24–36 towards the tidal inlets (Brambati, 1996). Small rivers, which

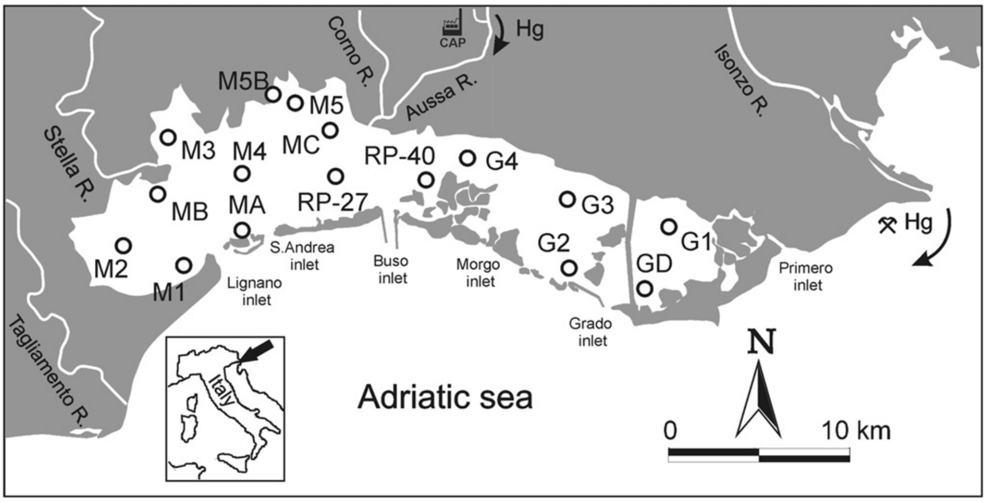

Fig. 1. Index map of the study area showing the locations of the sediment cores. The RP27 and RP40 core sites from Piani et al. (2005) are also included.

deliver water originating from groundwater, and from irrigation canals, flow into the lagoon. Particulate matter from these streams is of secondary importance. In fact, the primary source of suspended sediment is the sea, which delivers material from the Tagliamento and Isonzo River deltas, and from the erosion of the barrier islands. Dispersion of sediments into the lagoon is controlled by tidal fluxes through tidal inlets, where medium to fine sands are present, whereas the fine muddy component is widely dispersed throughout the inner basin, reaching the mudflats (Brambati, 1970).

Despite its high degree of vulnerability to the surrounding human pressures of urbanisation and industry, the lagoon system is one of the best conserved wetlands in the whole of the Mediterranean. One such example of nearby industry is the Torviscosa industrial complex, located in the Aussa-Corno River drainage basin. Although the discharge of wastewater has been under control since 1984, when clean-up technologies were introduced (RAFVG, 1991), contaminated run-off from the industrial site still finds its way into the river system. In addition, the lagoon, like the whole of the northeastern most region of Italy, was highly affected by radioactive fallout of ^{137}Cs following the Chernobyl nuclear accident in 1986, due mainly to the fact that this area experiences heavier rainfall than the rest of Italy. Ever since the accident, this area has been the focus of much related research, and is considered a final sink of ^{137}Cs, as well as metals (Belli et al., 1997; Piani and Covelli, 2001). Considering the high degree of contamination, as well as the problems for navigation along the channels due to sediment accumulation, the Decree of the President of the Council of Ministers of the Italian Government declared a state of socio-economic and environmental emergency in the Marano and Grado Lagoon in 2002. A Deputy Commissioner was then appointed to implement a series of restoration measures to address these issues and solve the emergency. These measures comprise several approaches that are still ongoing; for example, the reclamation of polluted areas, the improvement of water circulation and navigability in the lagoon channels, and environmental monitoring.

3. Materials and methods

3.1. Sediment cores

Sediment cores were collected in June and July 2008 with an in-house corer by hand-pushing plastic tubes (10 cm in diameter, 140 cm in length) into the bottom sediments. Coring sites were carefully selected within subtidal and intertidal areas belonging to each of the six lagoon sub-basins (Dorigo, 1965), distant from any tidal channel. Core M5B was collected in a saltmarsh. In addition, shallow sediment cores (8 cm diameter, 50 cm length) were also recovered using a light gravity “Kajak” corer (KC Denmark) coupled with acrylic liners. These smaller cores were used to determine age and calculate sediment accumulation rates for the past 50–150 years by measuring ^{137}Cs- and ^{210}Pb-activity depth profiles. The retrieved cores were sealed on board the boat, transported to the lab and stored at +4 °C in a cold room until further analysis.

All the cores were X-ray-radiographed to identify faint sedimentary structures, slight changes in density, texture and mineralogical composition and bioturbation. The adopted methodology was established following a review of previous studies (e.g. Bouma, 1964; Baker and Friedman, 1969). The X-ray source was a Balteau Baltospot GFD 300/5 directional generator. The film used was an Agfa Structurix D4 industrial x-ray film (10 × 48 cm format). The films were processed using an Agfa-Gevaert Structurix NDT E Processor, with a running time of 15 min and, subsequently, scanned for visual inspection of the images.

3.2. Core subsampling

After X-ray scanning, the longer cores were split using a rotating disk saw, photographed and visually described for lithology and colour variability (Munsell Soil Color Charts, 1975), as well as for sedimentary structures and macrofossil content. Subsampling was performed by cutting 1-cm-thick slices. Each sediment slice was split into several aliquotes for the analysis of grain size, water content, organic and total carbon (C_{org} and C_{tot}), total nitrogen (N_{tot}) and mercury (Hg) content. The analyses were performed at depth intervals of 0–1, 1–2, 5–6 and 9–10 cm, every 10 cm between 20 and 50 cm depth, at an intermediate depth between 50 cm and the core bottom, and at the core bottom itself.

3.3. Physical and geochemical analyses of the core sediments

For grain-size analysis, sediment samples were treated for 48 h with hydrogen peroxide (H_2O_2) to remove organic matter, and subsequently wet-sieved through a 2-mm sieve. The analyses were conducted on 2-mL samples using a Malvern Mastersizer 2000 laser granulometer. Porosity (Φ) was calculated by measuring the weight loss of sediments dried overnight at 110 °C (Loring and Rantala, 1992) to constant weight. The following equation (Johnson et al., 1982) was applied:

$$\Phi = (M_W/\rho_W)/(M_S/\rho_S) + (M_W/\rho_W),$$

where M_W is the weight of water lost; M_S is the weight of dry sediment; $\rho_W = 1.025$ g cm^{-3} is the water density; ρ_S is the sediment density measured from samples using a Micromeritics AccuPyc 1330 Picnometer.

The analyses of total and organic carbon (C_{tot} and C_{org}), and total nitrogen (N_{tot}) in freeze-dried (CoolSafe 55-4 SCANVAC) and homogenized sediment samples were performed using a Perkin Elmer 2400 CHN Elemental Analyzer after acidification of samples with 1 M HCl (Hedges and Stern, 1984) at a combustion temperature of 975 °C. The detection limit for C_{org} and C_{tot} was 0.1%. The precision for C_{tot}, C_{org}, and N_{tot} was 3%.

The determination of total mercury (Hg) in sediments was achieved using the total digestion method, recommended by Loring and Rantala (1992). About 200 mg of freeze-dried, pulverized and homogenized sediment was treated with a mixture of 1.5 mL HF + 5 mL *aqua regia* in a closed microwave system (Milestone MLS 1200). The solutions obtained were analyzed through the CVAAS technique (Perkin Elmer AAnalyst 100-FIAS) after a reduction step ($NaBH_4$ 3% in NaOH 1%). Quality control was tested using certified reference materials (PACS-2 harbour sediment, NCR-CNR, Canada; accepted value = 3.04 ± 0.20 mg kg^{-1}). The mean concentration of Hg in PACS-2 was 3.22 ± 0.10 mg kg^{-1}. The detection limit was 0.13 μg g^{-1}.

3.4. Radiometric analyses

Four of the smaller sediment cores (MB, M4, M5B and G3) were selected on the basis of their location and minimal bioturbation in the sedimentary sequence. Sediment cores were precisely extruded at 1 cm intervals. Sediment samples were weighed wet, then dried at 60 °C to constant weight, in order to determine wet and dry bulk density, according to Berner (1971), and assuming a sediment density of 2.55 g cm^{-3}. Dried sediment was then slightly disaggregated and analysed for radiotracers. ^{137}Cs was measured via gamma spectrometry (Frignani et al., 1991) using coaxial intrinsic germanium detectors. The disaggregated samples were put in plastic jars to obtain a number of standard geometries, and the abundance of the ^{137}Cs was measured using the peak at 661.7 keV.

The ^{137}Cs activity peaks, corresponding to 1963 and 1986, were used to infer mean accumulation rates, although the distribution of ^{137}Cs in sediment cores can also be forced by biomixing and molecular diffusion (Frignani et al., 2004).

^{210}Pb activity was measured via alpha-counting of its daughter, ^{210}Po, and assuming secular equilibrium between the two isotopes. ^{210}Po was extracted from the sediment with hot HNO_3 and H_2O_2, spiked with ^{209}Po used as a yield monitor for calculating the efficiencies. After separation of the leachate from the residue, the solution was evaporated to near dryness and HNO_3 was eliminated using concentrated HCl. The residue was dissolved in 1.5 N HCl. Iron was reduced using ascorbic acid and Po was plated onto a silver disk overnight, at room temperature. The two Po isotopes were alpha-counted using a silicon barrier detector coupled with a multichannel analyzer. The estimated analytical error varied from 5 to 10%. The method is reported by Frignani and Langone (1991) and discussed in detail by Frignani et al. (1993). Excess ^{210}Pb ($^{210}Pb_{ex}$) was calculated from the difference between total and supported ^{210}Pb. The value of supported ^{210}Pb activity was assumed constant throughout the core and estimated from the values of the deepest sediment samples, where ^{210}Pb was assumed to be in radioactive equilibrium with its parent ^{226}Ra. The supported ^{210}Pb values ranged between 15.7 and 21.2 Bq kg^{-1}, with no obvious spatial trend. The age of sediments and estimates of sediment accumulation rates were determined by applying a Constant Flux–Constant Sedimentation model (Robbins, 1978) to the activity-depth profile of excess ^{210}Pb, below the surface mixed layer. A more sophisticated conceptual model, the Constant Rate of ^{210}Pb Supply (CRS) model, was used on core M5B in order to estimate the changes of sediment accumulation rate over time (Robbins, 1978; Appleby and Oldfield, 1978, 1983).

4. Results

4.1. Core lithology

According to Shepard's classification (1954), core sediments are mainly dominated by sandy silt or silt; whereas, only sporadically, clayey silt is present. In the eastern sector of the lagoon, only the G2 and GD core profiles showed a clear decreasing trend of the sandy content from the core top downwards: 52.8 to 1.9% and 49.6 to 25.2%, respectively (Fig. 2). The decrease in sand along the profile was generally followed by an increase in silt. The silty fraction ranged between 26.7 and 74.8%. The clayey component was usually secondary, since its range was narrow, between 5.0 and 19.8%.

In the western sector (Fig. 3), subsuperficial sediments generally comprised silty sand, sandy silt, or silt, with a few exceptions in core MA (level 49–50 and 87–88.5 cm, sand) and M2 (39–40 and 98–99 cm, clayey silt). The amount of sand was related to the location of the sampling sites: cores M1 and MA, close to the barrier islands and to the main tidal channels, showed the highest content, between 64.4 and 76.2%. Conversely, cores collected from inner sectors, such as M3 and M5, yielded lower fractions of sand, ranging from 10.9 to 14.2%. Likewise, taking into consideration sediment mean size (Mz), a decrease from about 8 to about 4 μm was generally observed from the tidal inlets to the inner coastline of the lagoon.

4.2. Inorganic and organic carbon and total nitrogen core profiles

C_{inorg} content, which ranged from 2.73% (G3 69–70 cm) to 7.24% (GD 1–2 cm) in the Grado Lagoon and from 1.30% (M3 83–84 cm) to 8.05% (MA 1–2 cm) in the Marano Lagoon, reflects the prevailing carbonate origin of the sediments supplied to the coastal area by the two main tributary rivers, the Isonzo and Tagliamento (Brambati, 1969). C_{inorg} profiles followed the variability of the sandy component in those cores where this component was more abundant and/or more variable with depth (GD and G2 in the eastern sector; M1, MB and MA in the western sector, respectively). If all the analyzed core levels are considered, a significant positive correlation ($r = 0.713$, $n = 103$, $p < 0.001$) is found between the coarser component and the amount of C_{inorg} in the sediments. This also means that those sampling stations characterized by less active hydrodynamics and affected by low sandy content show the lowest amounts of C_{inorg}, which accounts for about 3% when no sand is present.

Excluding core M5B, where C_{org} concentrations were comparable to C_{inorg} content, the organic component of carbon was one order of magnitude lower than the inorganic component. Core M5B was the only one collected in a saltmarsh covered by halophytes and inundated during high spring tide events. Here, C_{org} concentrations in the first 10 cm were among the highest recorded in the cores (2.00–2.72%), decreasing down-core almost exponentially. In the remaining sediment cores, C_{org} concentrations varied between 0.32% (MA 1–2 cm) and 2.48% (G3 69–70 cm), with an average value of 1.22 ± 0.49%. An increase of C_{org} content in the intermediate core levels was often observed in all sites, and can be visually correlated to irregular thin peaty lenses or pockets of organic matter. C_{org} concentrations were positively correlated with mud content, although the correlation coefficient was rather low ($r = 0.531$, $p < 0.001$) due to local concentrations of organic matter in association with the already mentioned peaty lenses.

Nitrogen concentrations (0.02–0.29%, avg. 0.13 ± 0.06%) generally decreased from subsurface levels downwards, but irregular increases in N_{tot} content with depth were also observed (G2, GD, M4, MB, MC), with no obvious spatial pattern. The C_{org}/N_{tot} molar ratio is usually reported as an index for discriminating marine from terrestrial sources of organic matter. In the present study, C_{org}/N_{tot} values were mainly low (7.1–11.9) at the core top, increasing up to about 20 down-core. This trend was mainly due to low N_{tot} values, which are affected by early diagenesis processes related to faster nitrogen compound degradation, rather than an increase in C_{org} content. There were a few exceptions for the middle sections of some cores (G3, G4, M5B) located in low-energy sectors of the lagoon and close to the inner coastline. Here, C_{org}/N values reached up to about 35, corresponding to significant preserved terrestrial C_{org} content in peaty lenses compared to N content.

4.3. Mercury core profiles

Hg profiles in all cores (Figs. 2 and 3) showed a typical trend of an increase in metal concentration from the basal core sections, where local background values were found, to the top core sections. This increase frequently culminated in the highest Hg content being found in the uppermost core section. The profiles clearly reflect the contamination that has affected the area's more recent history, which has been well recorded into the lagoon sediments. Similar trends have also been found in some deep cores collected from the Isonzo River prodelta in the nearby Gulf of Trieste (Covelli et al., 2001, 2006b). Here, the vertical profiles of Hg content were demonstrated to be undoubtedly related to cinnabar ore extraction activity at the Idrija mine. Similarly, Gosar and Žibret (2011) also identified overbank sediment profiles in the Idrijca River valley as contamination hotspots. These deposits are eroded during high discharge events and represent a risk for further contamination in the drainage basin, and subsequently in the nearby northern Adriatic coastal environment.

The natural background level of Hg adopted here for the Marano and Grado Lagoon was 0.13 ± 0.04 μg g^{-1}, which corresponds to the

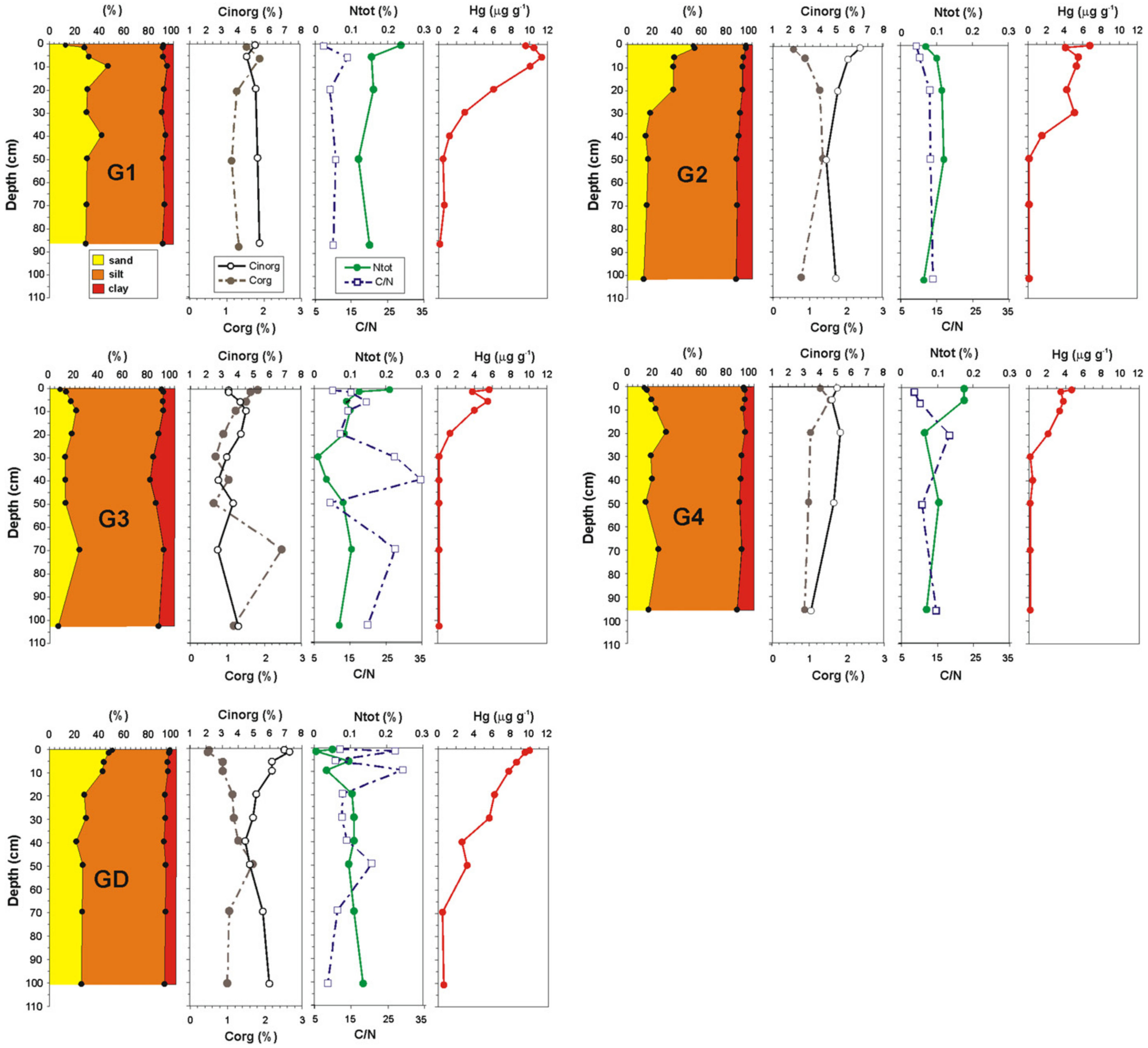

Fig. 2. Vertical profiles of grain size, C_{inorg}, C_{org}, N_{tot}, C_{org}/N_{tot} molar ratio and Hg in cores collected from the eastern sector of the basin (Grado Lagoon).

average Hg concentration reported for the basal sections of cores GT1, GT2 and GT3, collected from the Gulf of Trieste (Covelli et al., 2006b). In cores G2 and G4 (Grado Lagoon) and M5, MA and MC (Marano Lagoon), the background value was reached at a depth of 49–50 cm. The same value was found at greater depths in cores M5B (62–63 cm), M3 and M4 (69–70 cm) and G1 (86–87 cm). Conversely, preindustrial levels of Hg appeared at shallower depths in cores M1 (39–40 cm), MB and G3 (29–30 cm), and M2 (19–20 cm). Surprisingly, the background value was not reached even at a depth of 1 m in core GD (0.61 μg g^{-1}). However, this can be explained by taking into account the sampling site location, which is close to a main lagoon channel and to a tidal inlet where the transport of sediments (especially the sandy fraction) by tidal fluxes is more effective. We cannot exclude the possibility of a reworking of the sedimentary sequence, although the clear exponential trend of Hg concentration makes this hypothesis unlikely. In the Grado Lagoon, maximum Hg content was found at the core top (0–1 cm). A notable exception was core G1, where the highest concentration of Hg within all cores (11.36 μg g^{-1}) was reached at a depth of 5–6 cm. In the Marano Lagoon, the highest concentrations were often below the core top, mainly at a depth of 5–6 cm, as in cores M1 (0.98 μg g^{-1}), M3 (2.76 μg g^{-1}) and MA (3.90 μg g^{-1}), but also at a depth of 1–2 cm, as in core MB (2.10 μg g^{-1}). At some sites, peaks were detected at greater depths: 6.49 μg g^{-1} at 9–10 cm in core M5; and, at 19–20 cm, 6.49 μg g^{-1} and 3.96 μg g^{-1} in cores MC and M5B, respectively.

4.4. Radionuclide profiles, sediment accumulation rates and geochronology

The activity-depth profiles of ^{137}Cs and ^{210}Pb are shown in Fig. 4. The short-lived radionuclides ^{210}Pb and ^{137}Cs were used to calculate

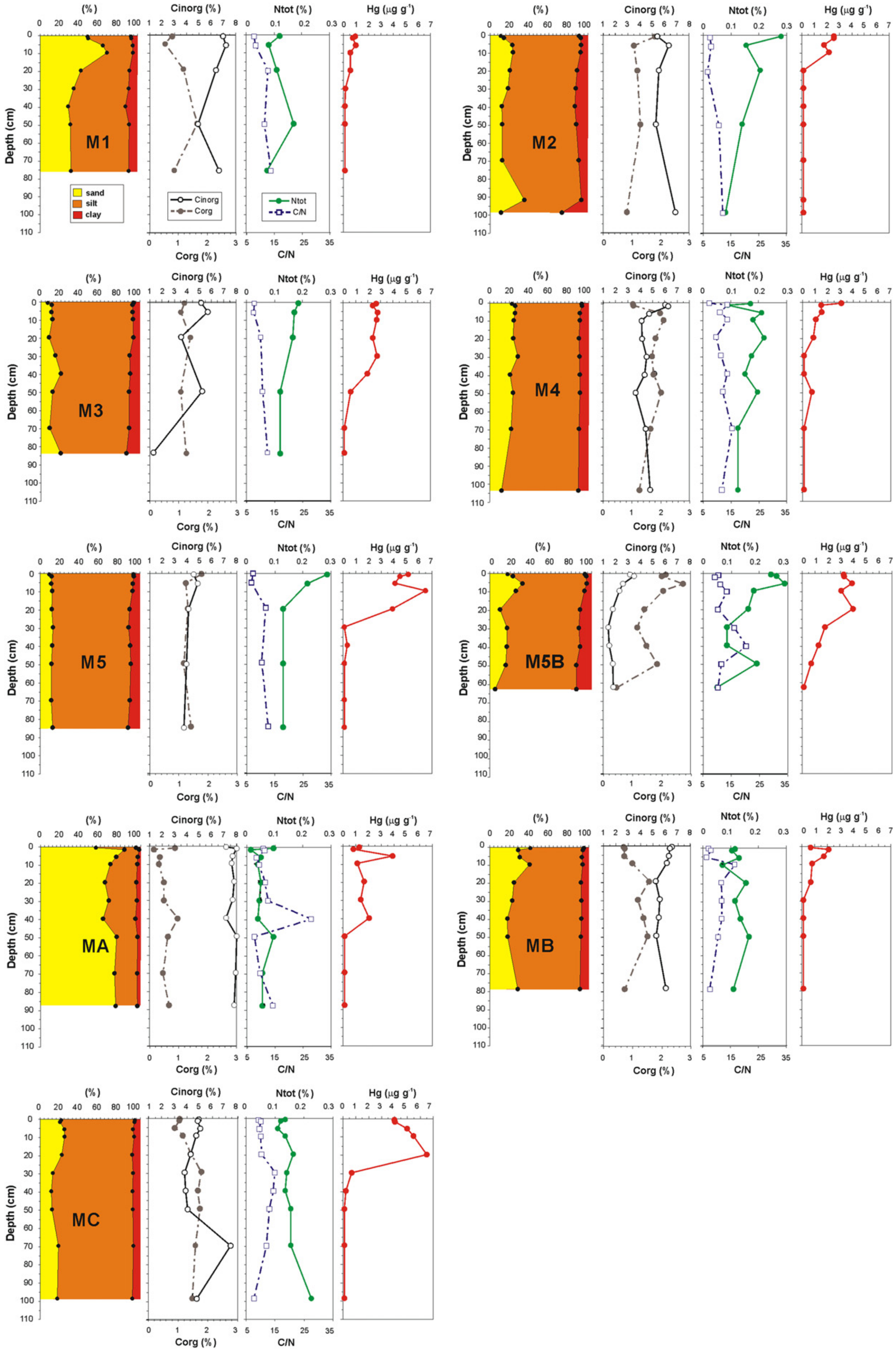

Fig. 3. Vertical profiles of grain size, C_{inorg}, C_{org}, N_{tot}, C_{org}/N_{tot} molar ratio and Hg in cores collected from the western sector of the basin (Marano Lagoon).

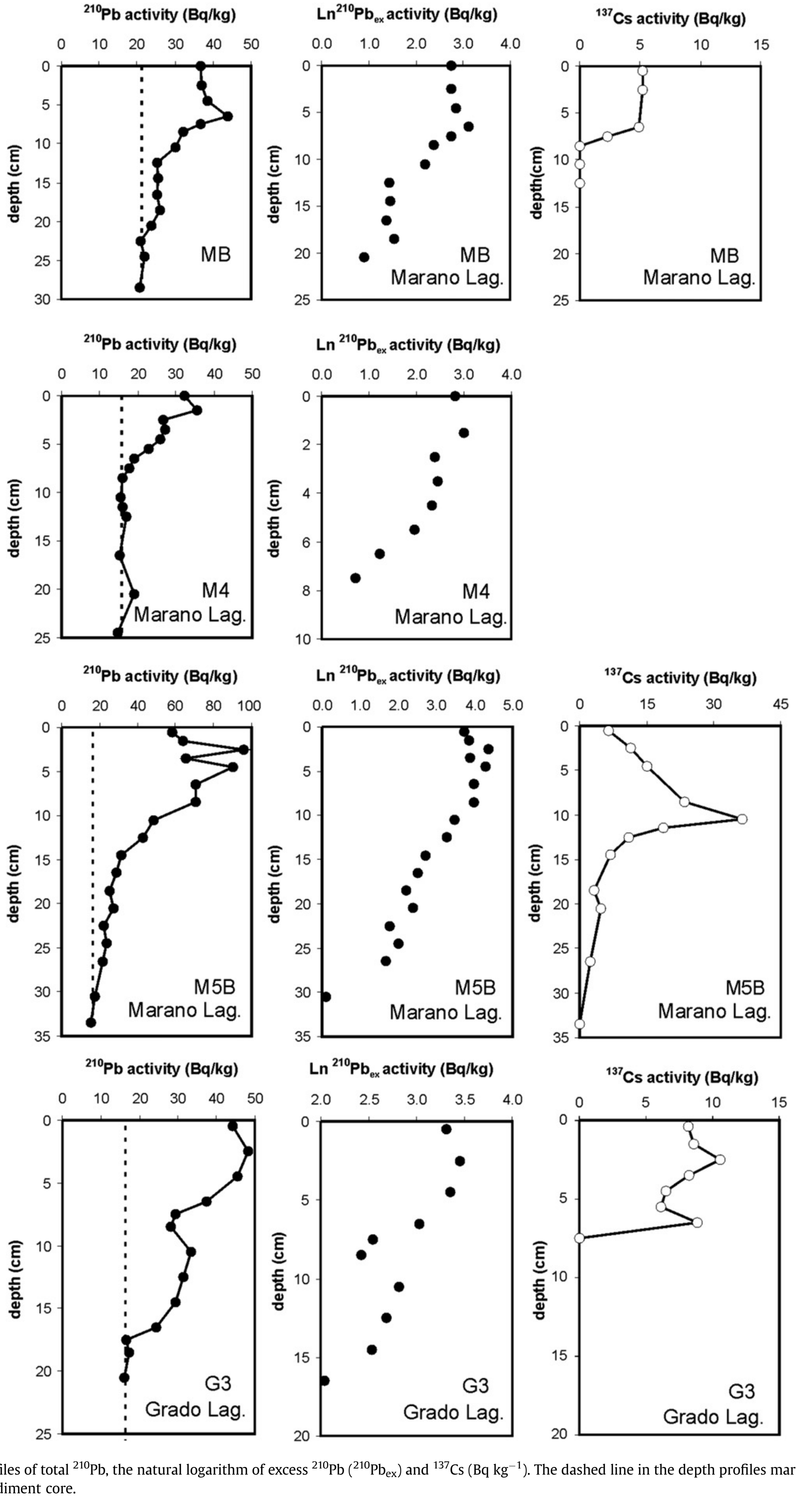

Fig. 4. Activity-depth profiles of total ^{210}Pb, the natural logarithm of excess ^{210}Pb (^{210}Pb$_{ex}$) and ^{137}Cs (Bq kg^{-1}). The dashed line in the depth profiles marks the background level of ^{210}Pb selected for each sediment core.

Table 1
Rates of sedimentation (S, cm y^{-1}) and mass accumulation (A, g cm^{-2} y^{-1}), calculated on the basis of ^{210}Pb and ^{137}Cs at four selected stations. CF–CS refers to results based on the Constant Flux–Constant Sedimentation model; the core region where the best-fit linear regression was applied is specified in parentheses; CRS refers to results based on the Constant Rate of ^{210}Pb Supply; and n.d. stands for 'not determined'.

Core	S_{210Pb} (cm y^{-1})	A_{210Pb} (g cm^{-2} y^{-1})	^{210}Pb method	S_{137Cs} (cm y^{-1})	^{137}Cs method
MB	0.12	0.15	CF–CS (6–13 cm) $n = 5$	0.13	^{137}Cs onset
M4	0.083	0.072	CF–CS (1–8 cm) $n = 6$	n.d.	n.d.
M5B	0.41	0.37	CRS (0–5 cm) $n = 5$	0.48	Chernobyl peak
	0.24	0.22	CRS (>5 cm) $n = 11$		
	0.26	*0.24*	CF–CS (8–27 cm) $n = 10$		
G3	0.13	0.097	CF–CS (3–9 cm) $n = 4$	0.11	Chernobyl peak
				0.13	^{137}Cs onset

sediment accumulation rates for approximately the last 50–150 years. ^{210}Pb ($t_{1/2} = 22.3$ y) is a naturally-occurring radionuclide originated from the ^{238}U series, which has been widely used as a geochronometer for age-dating on a 100-y timescale. ^{137}Cs ($t_{1/2} = 30.2$ y) is an artificial radionuclide supplied to aquatic environments by fallout from atomic weapons testing and via discharge from nuclear power plants. Radioactive fallout from atomic tests began in 1954 and peaked in 1963. The Chernobyl accident in April 1986 produced a new input of ^{137}Cs, easily recognizable in the northern Adriatic sediments. Although ^{137}Cs is affected by a greater mobility in the marine environment with respect to ^{210}Pb, it is commonly used as an independent method to confirm ^{210}Pb-based estimates of sediment accumulation rates. In the present study, ^{210}Pb activity in the cores decreased exponentially with depth, but with frequent oscillations (Fig. 4), implying non-steady-state sedimentation conditions. All cores showed a surface mixed layer, up to 6 cm thick in core MB. Some intermediate core intervals were characterized by *quasi*-vertical ^{210}Pb profiles (e.g. core MB, 12–19 cm). In these circumstances, multiple mechanisms (e.g. episodic and rapid depositional events, storm resuspension, bioturbation activity) drive the ^{210}Pb profile formation and hence the delivery of sedimentary material and ^{210}Pb to the bottom. In order to calculate a mean sediment accumulation rate for each core, we used the Constant Flux–Constant Sedimentation model (Robbins, 1978) and a best-fit linear regression was applied to the core region with more regularly decreasing activity, thus discarding data from the surface mixed layer or from quasi-vertical intervals.

In the central part of the Marano Lagoon (core M4), the mean sediment accumulation rate was very low (0.083 cm y^{-1}) (Table 1). Based on this estimate, the Chernobyl peak should be confined within the uppermost 2 cm and the maximum ^{137}Cs penetration should not exceed 4 cm. Hence, we decided not to count ^{137}Cs in that core. Core MB, collected in front of the Stella River mouth, gave a ^{210}Pb-based sediment accumulation rate of 0.12 cm y^{-1}. The ^{137}Cs profile did not show the peaks associated with maximum fallout (1963 and 1986); however, based on the depth of ^{137}Cs activity onset (7 cm) relative to 1954, a value of 0.13 cm y^{-1} was calculated, which supports the ^{210}Pb estimate very well. Core G3, collected from the centre of the Grado Lagoon, showed the most complex ^{210}Pb profile. A surface mixed layer and several down-core fluctuations were noticeable, changing in parallel according to porosity and grain size. Furthermore, the 10–15 cm interval was highly bioturbated by the abundant presence of bivalves. The sediment accumulation rate was thus calculated by using only the region between 3 and 9 cm, resulting in a value of 0.13 cm y^{-1}. Based on the onset of ^{137}Cs (1954), this estimate was confirmed. In addition, assuming the modest ^{137}Cs peak measured at a depth of 2.5-cm as a consequence of the Chernobyl accident, a sediment accumulation rate of 0.11 cm y^{-1} could then be calculated, which supports the previous estimates quite well. In the uppermost 5 cm of core M5B, ^{210}Pb activity was variable, whereas below that level it declined exponentially. Applying the CF–CS model in the deeper part of the ^{210}Pb profile, a mean sediment accumulation rate of 0.26 cm y^{-1} was calculated, whereas ^{137}Cs provided an estimate of 0.48 cm y^{-1}.

The apparent mismatch between the estimates of sediment accumulation rate obtained through the ^{210}Pb and ^{137}Cs profiles in core M5B (0.26 vs. 0.48 cm y^{-1}, respectively) requires some consideration of the assumptions in the dating model applied. The CF–CS provides an estimate of the sedimentation rate averaged over the last century, whereas the figure calculated from the Chernobyl peak of ^{137}Cs refers to a mean value for the last 20 years. To reconcile the results of the two methods, the sediment accumulation rate could have increased over time. The CF–CS model is probably not appropriate to calculate the sediment accumulation rate for this site, since it assumes that the flux of both ^{210}Pb and sediment has remained constant over time. In contrast, the CRS model assumes that the amount of sediment delivery may change over time, whereas the supply of ^{210}Pb is steady. Results of the CRS calculations for core M5B are shown in Fig. 5. The sedimentation rate remained fairly constant throughout the '900 (0.24 cm y^{-1}),

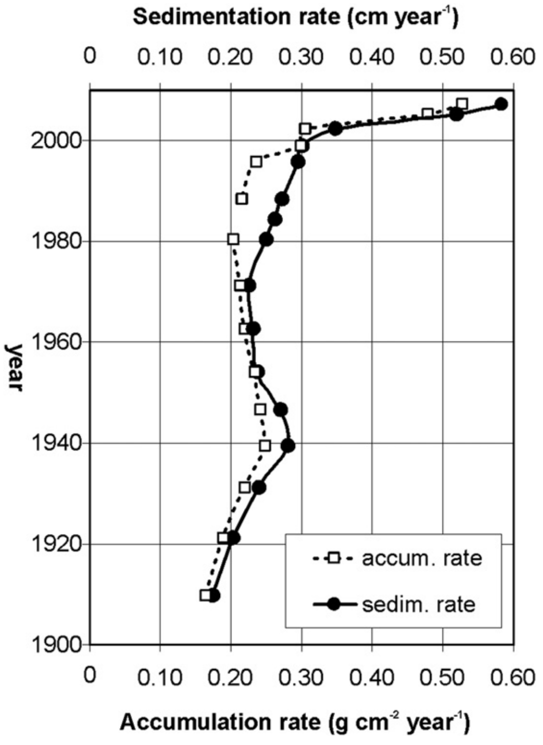

Fig. 5. Variability of the sedimentation rate (cm y^{-1}) and accumulation rate (g cm^{-2} y^{-1}) with time, calculated for core M5B by applying the CRS model to the ^{210}Pb profile.

then it rose sharply over the latest 10–20 years. Visual inspection and the porosity profile both revealed discontinuity at about a depth of 5 cm. It is possible that these features mark a change in the sedimentation regime, which occurred about 15 years before 2008 (based on CRS calculations). Core M5B was collected from a saltmarsh in the northern part of the Marano Lagoon, which is periodically flooded during high tide. In the northern Adriatic Sea, exceptional tide peaks are called *Acqua alta* and occur when the astronomical tides are reinforced by the prevailing winds (Scirocco and Bora), which hamper the usual reflux. The increase in accretion rate during the last 15 years might indicate a higher frequency of such events in recent years, as also reported for the Venice Lagoon (Bellucci et al., 2007). For the purposes of reconstructing the contamination history of Hg and other metals, we used a mean sediment accumulation rate of 0.24 cm y^{-1} from the core bottom up to a depth of 5 cm, and a value of 0.41 cm y^{-1} in the uppermost 5 cm. These values were calculated based on the CRS results and are in good agreement with the results obtained from the CF–CS model for the lower part of the sediment core and from the detection of the Chernobyl-related ^{137}Cs peak in the upper part of the core.

5. Discussion

5.1. Reconstructed mercury contamination history

Considering the absence of relevant post-depositional migrations or remobilization of Hg from bottom sediments after deposition, a geochronological reconstruction of Hg supply in recent sediments is possible. In particular, the anthropogenic component can be described by considering the productivity of the Idrija mercury mine and the more recent influence of the Torviscosa chemical complex as points of reference.

The depositional metal flux or accumulation rate (AR as mg Hg m^{-2} y^{-1}) can be calculated according to the relationship between Hg concentration (μg g^{-1}) in sediments $(Hg)_S$ and the accumulation rate of particles (ω, 10^{-1} g cm^{-2} y^{-1}), as in the following the equation:

$$\mathrm{HgAR} = \omega \bullet (\mathrm{Hg})_S,$$

where $\omega = (1 - \Phi) \bullet S \bullet \rho$, with Φ representing porosity, S the sedimentation rate (mm y^{-1}), and ρ the mean sediment density

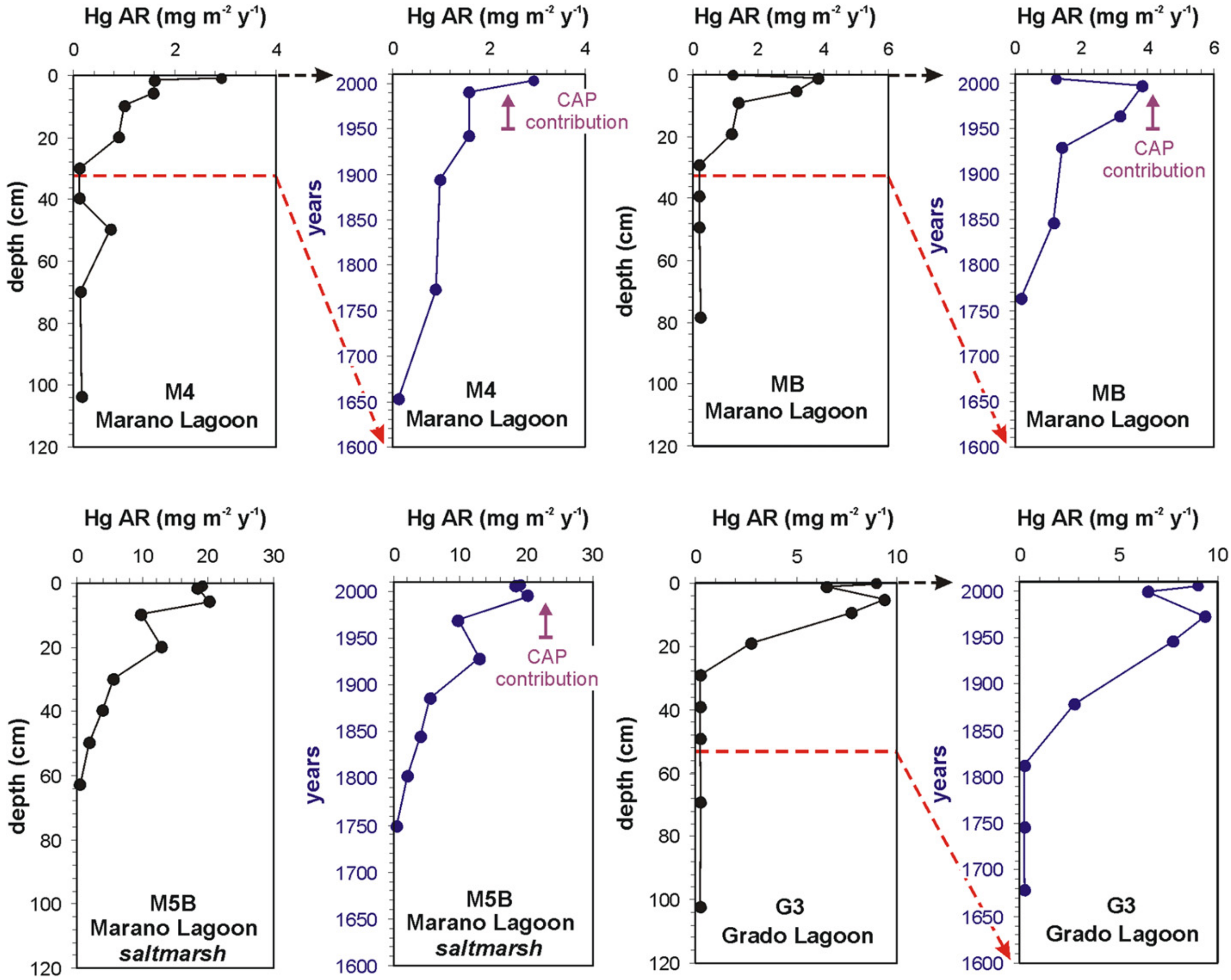

Fig. 6. Assessment of Hg fluxes (accumulation rate) in sediment cores collected from sampling stations MB, M4 and M5B (Marano Lagoon) and G3 (Grado Lagoon). The timescale was calculated on the basis of the sedimentation rates estimated for each site according to the ^{210}Pb activity-depth profile.

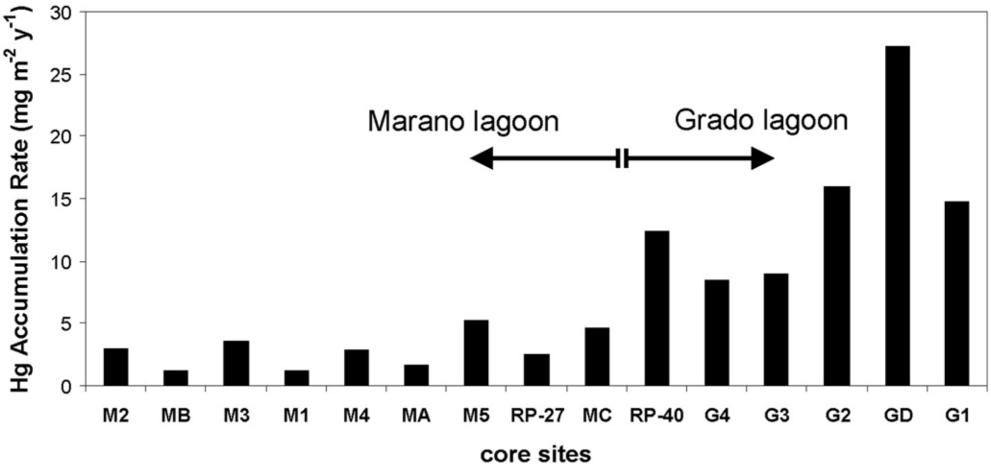

Fig. 7. Assessment of present annual fluxes (accumulation rate) of Hg, calculated for the first centimetre at all the sites sampled in the Marano and Grado Lagoon. Sedimentation rates used in these calculations were those measured at the three stations MB, M4 and G3 (see text for explanation). The present accumulation rate for the only core collected from a saltmarsh (M5B) is not reported. Conversely, sites RP-27 and RP-40, formerly considered by Piani et al. (2005) and re-sampled in this study, are included. Sampling sites are arranged from west (left) to east (right).

($g\ cm^{-3}$). The temporal variability of excess Hg due to anthropogenic activity can be assessed from the difference between total and natural (i.e. pre-extraction activity) Hg fluxes:

$$\text{HgAR}\ \textit{anthropogenic} = \text{HgAR}\ \textit{total} - \text{HgAR}\ \textit{natural}$$

Applying the average sedimentation rates estimated on the basis of ^{210}Pb activity in the uppermost 40 cm of cores MB, M4, M5B, and G3, and taking into account the vertical variability of porosity and density, accumulation rates were determined.

Vertical profiles with estimated age (Fig. 6) revealed that HgAR caused by anthropogenic activity is undoubtedly recorded in the lagoon's sediments, albeit in different ways across the various lagoon sectors. However, the key date seems to be around 1800, when the onset of the increase in anthropogenic HgAR in the eastern sector of the lagoon (Marano) at sites MB and M5B is apparent; whereas, at site M4 it is slightly older than that date. Although mining activity began at the end of the 15th century (Mlakar, 1974), the sediment cores showed no evidence of anthropogenic Hg enrichment until the sharp increase in activity at around 1800 AD, since the contribution of mining activity was probably insufficient to be recorded in the sedimentary sequence. One could also speculate that this is the time lag it takes for the lagoon system to respond to such activity. Therefore, one could also expect at least the same period of time (two centuries) for the lagoon to begin recording the accumulation of Hg-free sediments.

The increase in HgAR in the lagoon up until 1950 should only be attributed to longshore current dispersion of the Hg-rich Isonzo River suspended load, further to transportation and settling due to tidal fluxes. After that date, the occurrence of Hg in the uppermost part of the sedimentary sequence could be due to both sources, mining and industrial. This double origin was already reported in a speciation study conducted in the central sector of the lagoon by Piani et al. (2005). Cinnabar and non-cinnabar compounds were found to be present in the bottom sediments in different proportions, except for those samples collected inside the Aussa River (Fig. 1), where cinnabar was virtually absent. The present decrease in HgAR was only evident at site MB, along with a possible but uncertain result at site M5B. Conversely, the opposite trend was found at site M4 site, which is difficult to interpret. One possibility is that this site has recently been affected by the accumulation of resuspended contaminated sediment due to dredging operations in nearby tidal channels.

In the Grado Lagoon, at station G3, the onset of HgAR appeared slightly after 1800, peaking around 1971 and again around 2005, interrupted by a decrease in 1998. Considering the location of the G3 site, we can be confident that recent high HgARs can only be due to sedimentary supplies related to the mining activity at Idrija. Clearly then, in spite of the mine having closed about 15 years ago, there is no evidence of a subsequent gradual decrease in Hg flux at site G3. Although extreme flood events in the Isonzo River are infrequent, their contribution in terms of delivering particulate Hg into the Gulf of Trieste still remains considerable (Covelli et al., 2007). Washout of contaminated sediments from the mining region, from the Idrijca-Isonzo River drainage basin, where mining residues have been deposited over five centuries (Žibret and Gosar, 2006; Gosar and Žibret, 2011), provides Hg in particulate form to the river's discharge. Kocman et al. (2009) calculated that, owing to the resuspension of contaminated river sediments from the Idrijca River, between 200 and 800 kg of Hg can be expected to be transported out of the catchment area in a flood in a given

Table 2
Total and anthropogenic inventory of Hg for each sampling station, mean values and amount of Hg buried in the bottom sediments evaluated for each sub-basin.

	Lagoon sub-basin	Core	Total Hg Inv ($mg\ m^{-2}$)	Anthropogenic Hg Inv ($mg\ m^{-2}$)	Hg burial (t)
1	MARANO	M2	417	248	*29*
	5056 ha	M1	466	317	
		MB	399	334	
		M3	1529	1376	
		Mean	*703*	*569*	
2	S.ANDREA	M4	623	435	*19*
	2150 ha	MA	1511	1310	
		Mean	*1067*	*872*	
3	BUSO	M5	1959	1806	*59*
	3556 ha	MC	2085	1914	
		G4	1442	1257	
		Mean	*1829*	*1659*	
4	MORGO 297 ha	G2	2565	2369	7
5	GRADO	G3	1140	945	*88*
	3314 ha	G2	2565	2369	
		GD	4886	4694	
		Mean	*2864*	*2669*	
6	PRIMERO 1368 ha	G1	3708	3547	*49*

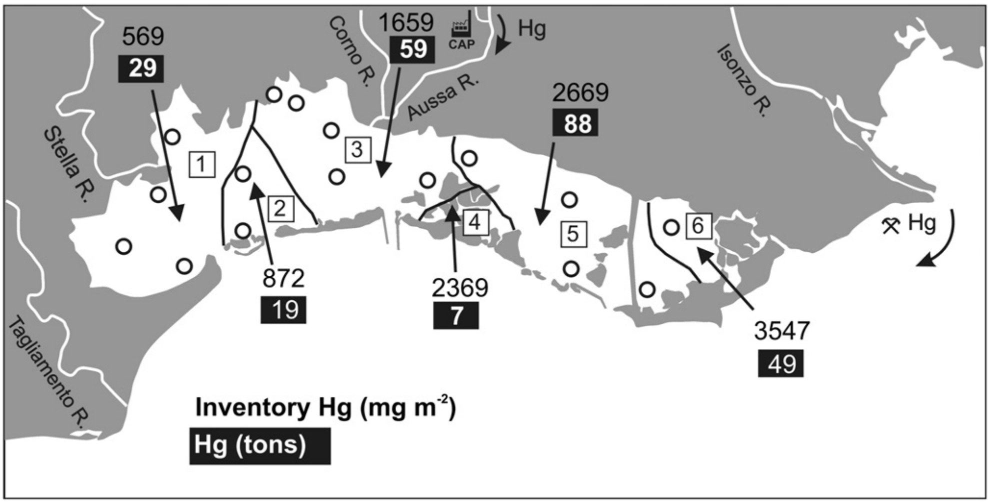

Fig. 8. Anthropogenic inventory and amount of Hg buried in bottom sediments for each of the six sub-basins of the Marano and Grado Lagoon.

hydrological year. A short-term drastic reduction of Hg input from the river basin into the Gulf of Trieste and the lagoon is unlikely in the foreseeable future. Therefore, natural remediation of contaminated marine and lagoon sediments due to Hg-free sedimentary supplies is equally unlikely, which in turn means that the current level of risk for biota of exposure to Hg will doubtless remain for an indefinite period of time.

A further estimation of the spatial variability of the recent HgARs can be made for all the core sites, taking into consideration the uppermost core level (0–1 cm). Although the activity-depth profiles of ^{137}Cs and ^{210}Pb were not determined for all sites, the sedimentation rates obtained for sites MB, M4 and G3 were applied according to the location of the cores relative to one of these three sites (i.e. M2 and M3 as MB; M1, MA, M5 and MC as M4; and G1, G2, G4 and GD as G3). The results clearly show that HgARs in the Grado Lagoon are of one order of magnitude higher than in the Marano Lagoon (Fig. 7), especially in the easternmost sector (GD, 27.21 mg Hg m^{-2} y^{-1}; G1, 15.91 mg Hg m^{-2} y^{-1}; G2, 14.82 mg Hg m^{-2} y^{-1}). Hg fluxes in the lagoon environment were found to be lower than the highest value reported for the Gulf of Trieste (Covelli et al., 2006b) in front of the Isonzo River delta (31.49 mg Hg m^{-2} y^{-1}), but they undoubtedly appeared higher than the Hg accumulation rate assessed for the more distal marine coastal area (1.77–4.23 mg Hg m^{-2} y^{-1}). Similar values were found for the western sector of the lagoon, where M5 (5.27 mg Hg m^{-2} y^{-1}), MC (4.72 mg Hg m^{-2} y^{-1}) and M3 (3.69 mg Hg m^{-2} y^{-1}) exhibited the highest rates, thus confirming these areas as preferential accumulation sites for Hg.

5.2. Mercury inventory

The cumulative Hg inventory quantifies the total amount of the metal loaded to the sediments over time and deposited on a 1 m^2 surface area (Kolak et al., 1998). An assessment of the anthropogenic Hg buried in the sedimentary column from when the mining activity commenced was attempted, applying the following equation:

$$\text{Hg Inv}\left(\text{mg m}^{-2}\right) = \sum\left[(\text{Hg}^*)_S \bullet (1-\varphi) \bullet \rho \bullet d\right],$$

where Hg* is the metal concentration corrected for the background value and d is the thickness of sediment between two consecutive analyzed core levels. Results showed significant differences between the two lagoon sectors. The accumulation of Hg was found to be more readily concentrated in the eastern part of the lagoon environment, the most affected by riverine Hg inputs. However, in the central sector, which is known as Buso Basin, sites MC and M5 revealed the largest inventory, thus suggesting a probable contribution of the Aussa-Corno River system to the level of Hg* accumulation in the bottom sediments (Piani and Covelli, 2001).

On the basis of the Hg* inventory, calculated for each core, a preliminary, rough estimation of the total amount of Hg accumulated in the sediments due to both sources, industrial and mining, was evaluated for each lagoonal sub-basin. It was evident that a greater number of core profiles would have increased the confidence level of the estimate of the spatial variability of the sedimentary sequence thickness where Hg content occurred above the background level. Besides, the area covered by saltmarshes (about 760 ha, 5% of the entire lagoon system; Fontolan et al., 2012) was not discerned in this preliminary calculation, which could have resulted in an underestimation of the overall amount of Hg buried in the lagoon, since saltmarshes are known to be even more efficient "traps" for sediment and associated contaminants (see M5B core profile) than tidal flats. Furthermore, no distinction was made for the navigation channels, where the sediment thickness contaminated by Hg is often larger than that reported for the subtidal zone due to the progressive and periodical silting-up of the channel bottom. In spite of these limitations, an assessment of the "reservoir" effect of the lagoon sediments related to Hg can be provided.

If we consider the mean Hg inventory for each single sub-basin (Table 2) and their extension according to Dorigo (1965), a preliminary rough estimation, approximate by defect, of the amount of Hg "trapped" in bottom sediments of the lagoon accounts for about 251 t (Fig. 8). Around 137 t are buried in the Grado and Primero basins, where Hg is exclusively related to the mining activity. Recent assessments of Hg stored in the Idrijca River valley account for 2029 t (Žibret and Gosar, 2006), whereas the total amount of Hg in riverbed, riverbanks and flood plains, as well as in storage basins between the town of Idrija and the Isonzo River mouth, has been estimated to be about 10,000 t (Žagar et al., 2006). At least 900 t could be buried in bottom sediments of the Gulf of Trieste according to Covelli et al. (2006b). These estimates represent small figures if compared to the overall 37,000 t of Hg that were lost into the environment during the five-century-long mining history, according to the most recent estimations (Dizdarevič, 2001). There is probably an underestimation of the total amount of Hg stored in the riverine as well as in the marine and lagoon sediments affected by the Isonzo River inputs, although the quantity of the metal dispersed in the rest of the Adriatic Sea is unknown.

6. Conclusions

The presence of Hg in the Marano and Grado Lagoon environment must be considered a permanent issue and the biogeochemical behaviour of this metal in the sediment–water system should be carefully considered in the future, especially when decisions are needed regarding new uses of lagoonal areas. The preliminary rounded-down gross estimate of total Hg "trapped" in the lagoon's sediments, along with the complexity of the lagoon ecosystem, suggests that an *in toto* reclamation of the sediments is unfeasible. A partial removal of contaminated sediments could be practicable, but only in selected and restricted areas, such as inside fish farms; however, this kind of intervention is not broadly realistic across the lagoon as a whole from an economic or environmental perspective. Hence, if the bottom sediments of fish farms were to be dredged, this could guarantee total recovery for a certain number of years, but new contaminated sediments will keep being deposited, thus entering the fish farms during tidal fluxes. The remediation process would then be undermined if the water exchange with lagoon channels is not regulated through the use of sluice gates to stop the flow of water during flood events, intense wave motion and/or dredging operations in the lagoon channels. Accumulation rates of Hg could be even higher than they are currently, since dredging increases the space available to accommodate sediments, which would be "drained" into the fish farms.

On the other hand, dredging the lagoon channels is unavoidable if one wants to improve water circulation and navigability. Dredged sediments cannot simply be translocated to both sides of the channels, as it was in the past, since this practice is no longer allowed under national regulations. Some areas of this dredged sediment have been colonized by halophytes and, consequently, long-shaped saltmarshes have formed along the channels. Sediments contaminated by Hg (all forms) are currently dredged and disposed of in selected sites, both inland and along the inner margin of the lagoon, which are not connected to the lagoonal waters. Being able to keep the sediments in the lagoon would be a lot less expensive and, at the same time, the lagoon's sedimentary budget would be preserved. Demonstrating that this practice does not pose a threat in terms of Hg remobilization would be a great contribution towards changing the current national regulations, and thus represents a challenge for future research in this area.

Acknowledgements

The "MIRACLE" (Mercury Interdisciplinary Research for Appropriate Clam farming in Lagoon Environment") Project was supported financially by the Commissario Delegato for the Marano and Grado Lagoon in 2008–2009 (coordinator: S. Covelli). This is contribution No. 1750 from CNR-ISMAR Bologna. We wish to extend warm thanks to S. Caressa for his help with the sampling and fieldwork, and thanks are also due to M. Bussi and C. Landucci from DiGEO Trieste for their contribution to the grain-size and CHN analyses.

References

Appleby, P.G., Oldfield, F., 1978. The calculation of lead-210 dates assuming a constant rate of supply of unsupported ^{210}Pb to the sediment. Catena 5, 1–8.

Appleby, P.G., Oldfield, F., 1983. The assessment of ^{210}Pb data from sites with varying sediment accumulation rates. Hydrobiologia 103, 29–35.

Baker, S.R., Friedman, G.M., 1969. A non destructive core analysis technique using X-rays. Journal of Sedimentary Petrology 39, 1371–1383.

Belli, M., Colizza, E., Fanzutti, G.P., Finocchiaro, F., Melis, R., Piani, R., Sansone, U., 1997. The role of a spring river as a source of ^{137}Cs in a lagoon environment: the case of the Stella River (Marano lagoon, Northern Adriatic Sea). In: Desmet, G., et al. (Eds.), Freshwater and Estuarine Radioecology. Elsevier Science B.V., pp. 97–108.

Bellucci, L.G., Frignani, M., Cochran, J.K., Albertazzi, S., Zaggia, L., Cecconi, G., Hopkins, H., 2007. ^{210}Pb and ^{137}Cs as chronometers for salt marsh accretion in the Venice Lagoon – links to flooding frequency and climate change. Journal of Environmental Radioactivity 97, 85–102.

Benoit, J.M., Gilmour, C.C., Mason, R.P., Riedel, G.S., Riedel, G.F., 1998. Behaviour of mercury in Patuxent River estuary. Biogeochemistry 40, 249–265.

Benoit, J.M., Gilmour, C.C., Heyes, A., Mason, R.P., Miller, C.L., 2003. Geochemical and biological controls over methylmercury production and degradation in aquatic ecosystems. In: Biogeochemistry of Environmentally Important Trace Elements. ACS Symposium Series, vol. 835, pp. 262–297.

Berner, R.A., 1971. Principles of Chemical Sedimentology. McGraw–Hill, New York, 240 pp.

Bloom, N.S., Moretto, M.L., Ugo, P., 2004. A comparison of the speciation and fate of mercury in two contaminated coastal marine ecosystems: the Venice Lagoon (Italy) and Lavaca Bay (Texas). Limnology and Oceanography 2, 367–375.

Bouma, A.H., 1964. Notes on X-ray interpretation of marine sediments. Marine Geology 2, 278–309.

Brambati, A., 1969. Sedimentazione recente nelle Lagune di Marano e Grado (Adriatico settentrionale). Studi Trentini Scienze Naturali – Acta Geologica A XLVI, 142–239.

Brambati, A., 1970. Provenienza, trasporto e accumulo dei sedimenti recenti nelle lagune di Marano e Grado e nei litorali tra i fiumi Isonzo e Tagliamento. Memorie Società Geologica Italiana IX, 281–329.

Brambati, A., 1996. Metalli pesanti nelle Lagune di Marano e Grado. Piano di studi finalizzato all'accertamento della presenza di eventuali sostanze persistenti nelle Lagune di Grado e Marano e al loro risanamento, Regione Autonoma Friuli-Venezia Giulia, Direzione Regionale dell'Ambiente, Servizio dell'Idraulica, Trieste, p. 174.

Brambati, A., 2001. Coastal sediments and biota as indicators of Hg contamination in the Marano and Grado Lagoons. RMZ – Materials & Geoenvironment 48, 165–171.

Canário, J., Vale, C., Caetano, M., 2005. Distribution of monomethylmercury and mercury in surface sediments of the Tagus Estuary (Portugal). Marine Pollution Bulletin 50, 1142–1145.

Conaway, C.H., Watson, E.B., Flanders, J.R., Russell Flegal, A., 2004. Mercury deposition in a tidal marsh of south San Francisco Bay downstream of the historic New Almaden mining district, California. Marine Chemistry 90, 175–184.

Covelli, S., Horvat, M., Faganeli, J., Brambati, A., 1999. Porewater distribution and benthic flux of mercury and methylmercury in the Gulf of Trieste (northern Adriatic Sea). Estuarine, Coastal and Shelf Science 48, 415–428.

Covelli, S., Faganeli, J., Horvat, M., Brambati, A., 2001. Mercury contamination of coastal sediments as the result of a long-term cinnabar mining activity (Gulf of Trieste, Northern Adriatic sea). Applied Geochemistry 16, 541–558.

Covelli, S., Piani, R., Kotnik, J., Horvat, M., Faganeli, J., Brambati, A., 2006a. Behaviour of Hg species in a microtidal deltaic system: the Isonzo River mouth (northern Adriatic Sea). Science of the Total Environment 368, 210–223.

Covelli, S., Fontolan, G., Faganeli, J., Ogrinc, N., 2006b. Anthropogenic markers in the Holocene stratigraphic sequence of the Gulf of Trieste (northern Adriatic Sea). Marine Geology 230, 29–51.

Covelli, S., Piani, R., Acquavita, A., Predonzani, S., Faganeli, J., 2007. Transport and dispersion of particulate Hg associated to a river plume in coastal Northern Adriatic environments. Marine Pollution Bulletin 55, 436–450.

Covelli, S., Faganeli, J., De Vittor, C., Predonzani, S., Acquavita, A., Horvat, M., 2008. Benthic fluxes of mercury species in a lagoon environment (Grado lagoon, Northern Adriatic Sea, Italy). Applied Geochemistry 23, 529–546.

Covelli, S., Acquavita, A., Piani, R., Predonzani, S., De Vittor, C., 2009. Recent and past contamination of mercury in an estuarine environment (Marano lagoon, Northern Adriatic, Italy). Estuarine, Coastal and Shelf Science 82, 273–284.

Dizdarevič, T., 2001. The influence of mercury production in Idrija mine on the environment in the Idrija region and over a broad area. RMZ – Materials & Geoenvironment 48, 56–64.

Dorigo, L., 1965. La laguna di Grado e le sue foci. Ricerche e rilievi idrografici, vol. 155. Ufficio Idrografico del Magistrato alle Acque, Venezia, p. 231.

Fabbri, D., Locatelli, C., Snape, C.E., Tarabusi, S., 2001. Sulfur speciation in mercury-contaminated sediments of a coastal lagoon: the role of elemental sulfur. Journal of Environmental Monitoring 3, 483–486.

Faganeli, J., Horvat, M., Covelli, S., Fajon, V., Logar, M., Lipej, L., Cermelj, B., 2003. Mercury and methylmercury in the Gulf of Trieste (northern Adriatic sea). Science of the Total Environment 304, 315–326.

Fitzgerald, W.F., Lamborg, C.H., Hammerschmidt, C.R., 2007. Marine biogeochemical cycling of mercury. Chemical Reviews 107, 641–662.

Fontolan, G., Pillon, S., Bezzi, A., Villalta, R., Lipizer, M., Triches, A., D'Aietti, A., 2012. Human impact and the historical transformation of saltmarshes in the Marano and Grado Lagoon, northern Adriatic Sea. Estuarine, Coastal and Shelf Science 113, 41–56.

Frignani, M., Langone, L., 1991. Accumulation rates and ^{137}Cs distribution in sediments off the Po River delta and the Emilia-Romagna coast (northwestern Adriatic Sea, Italy). Continental Shelf Research 11, 525–542.

Frignani, M., Langone, L., Ravaioli, M., Sticchi, A., 1991. Cronologia di sedimenti marini. Analisi di radionuclidi naturali ed artificiali mediante spettrometria gamma. IGM-CNR Technical Report 24, p. 32.

Frignani, M., Langone, L., Albertazzi, S., Ravaioli, M., 1993. Cronologia di sedimenti marini. Analisi di ^{210}Pb via ^{210}Po per spettrometria alfa. IGM-CNR Technical Report 28, p. 24.

Frignani, M., Sorgente, D., Langone, L., Albertazzi, S., Ravaioli, M., 2004. Behaviour of Chernobyl radiocesium in sediments of the Adriatic Sea offshore the Po River delta and the Emilia-Romagna coast. Journal of Environmental Radioactivity 71, 299–312.

Gagnon, C., Pelletier, E., Mucci, A., 1997. Behaviour of anthropogenic mercury in coastal marine sediments. Marine Chemistry 59, 159–176.

Gosar, M., Žibret, G., 2011. Mercury contents in the vertical profiles through alluvial sediments as a reflection of mining in Idrija (Slovenia). Journal of Geochemical Exploration 110, 81–91.

Hammerschmidt, C.R., Fitzgerald, W.F., 2008. Sediment–water exchange of methylmercury determined from shipboard benthic flux chambers. Marine Chemistry 109, 86–97.

Hedges, J.I., Stern, J.H., 1984. Carbon and nitrogen determinations in carbonate-containing solids. Limnology and Oceanography 29, 657–663.

Horvat, M., Covelli, S., Faganeli, J., Logar, M., Mandic, V., Rajar, R., Sirca, A., Zagar, D., 1999. Mercury in contaminated coastal environment; a case study: the Gulf of Trieste. Science of the Total Environment 237/238, 43–56.

Johnson, T.C., Evans, J.E., Eisenreich, S.J., 1982. Total organic carbon in Lake Superior sediments: comparison with hemipelagic and pelagic marine environments. Limnology and Oceanography 15, 958–960.

Kading, T.J., Mason, R.P., Leaner, J.J., 2009. Mercury contamination history of an estuarine floodplain reconstructed from a ^{210}Pb-dated sediment core (Berg River, South Africa). Marine Pollution Bulletin 59, 116–122.

Kocman, D., Kanduč, T., Ogrinc, N., Kotnik, J., Horvat, M., 2009. Distribution and partitioning of Hg between water, suspended matter and bottom sediments of the Idrijca River, Slovenia. In: Abstracts book – 9th International Conference on Mercury as a Global Pollutant, Guiyang, Guizhou, China, 7–12 June 2009. GUIYANG: Institute of Geochemistry, Chinese Academy of Sci., S12, p. 69.

Kolak, J.J., Long, D.T., Beals, T.M., 1998. Anthropogenic inventories and historical and present accumulation rates of copper in Great Lakes sediments. Applied Geochemistry 13, 59–75.

Lawson, N.C., Mason, R.P., 1998. Accumulation of mercury in estuarine food chains. Biogeochemistry 40, 235–247.

Loring, D.H., Rantala, R.T.T., 1992. Manual for the geochemical analyses of marine sediments and suspended particulate matter. Earth-Science Reviews 32, 235–283.

Mason, R.P., Lawrence, A.L., 1999. Concentration, distribution, and bioavailability of mercury and methylmercury in sediments of Baltimore Harbor and Chesapeake Bay, Maryland. Environmental Toxicology and Chemistry 18, 2438–2447.

Mlakar, L., 1974. An outline of production of the Idrija mercury mine through the centuries. Idrijska Razgledi 3–4, 1–115.

Morel, F.M.M., Kraepiel, A.M.L., Amyot, M., 1998. The chemical cycle and bioaccumulation of mercury. Annual Review of Ecology and Systematics 29, 543–566.

Munsell Soil Color Charts, 1975. Macbeth Division of Kollmorgen Corporation, Baltimore, Maryland.

Muresan, B., Cossa, D., Jézéquel, D., Prévot, F., Kerbellec, S., 2007. The biogeochemistry of mercury at the sediment-water interface in the Thau lagoon. 1. Partition and speciation. Estuarine, Coastal and Shelf Science 72, 472–484.

Piani, R., Covelli, S., 2001. Contributo antropico di metalli pesanti e ^{137}Cs nei sedimenti del bacino di Buso (Laguna di Marano e Grado, Italia settentrionale). Studi Trentini Scienze Naturali – Acta Geologica A 77, 169–177.

Piani, R., Covelli, S., Biester, H., 2005. Mercury contamination in Marano Lagoon (Northern Adriatic sea, Italy): source identification by analyses of Hg phases. Applied Geochemistry 20, 1546–1559.

Point, D., Monperrus, M., Tessier, E., Amouroux, D., Chavaud, L., Thouzeau, G., Jean, F., Amice, E., Grall, J., Leynaert, A., Clavier, J., Donard, O.F.X., 2007. Biological control of trace metal and organometal benthic fluxes in a eutrophic lagoon (Thau lagoon, Mediterranean Sea, France). Estuarine, Coastal and Shelf Science 72, 457–471.

RAFVG, 1991. La qualità delle acque della Laguna di Marano. Regione Autonoma Friuli Venezia Giulia, USL 8. Regional Technical Report, Udine, 1991, p. 101.

Robbins, J.A., 1978. Geochemical and geophysical application of radioactive lead. In: Nriagu, J.O. (Ed.), The Biogeochemistry of Lead in the Environment. Elsevier, Amsterdam, pp. 285–393.

Ruiz-Fernández, A.C., Frignani, M., Hillaire-Marcel, C., Ghaleb, B., Arvizu, M.D., Raygoza-Viera, J.R., Páez-Osuna, F., 2009. Trace metals (Cd, Cu, Hg, and Pb) accumulation recorded in the intertidal mudflat sediments of three coastal lagoons in the Gulf of California, Mexico. Estuaries and Coasts 32, 551–564.

Sager, D.R., 2002. Long-term variation in mercury concentrations in estuarine organisms with changes in releases into Lavaca Bay, Texas. Marine Pollution Bulletin 44, 807–815.

Shepard, F.P., 1954. Nomenclature based on sand-silt-clay ratios. Journal of Sedimentary Petrology 24, 151–158.

Shi, J.-b., Ip, C.C.M., Zhang, G., Jiang, G.-b., Li, X.-d., 2010. Mercury profiles in sediments of the Pearl River Estuary and the surrounding coastal area of South China. Environmental Pollution 158, 1974–1979.

Trombini, C., Fabbri, D., Lombardo, M., Vassura, I., Zavoli, E., Horvat, M., 2003. Mercury and methylmercury contamination in surficial sediments and clams of a coastal lagoon (Pialassa Baiona, Ravenna, Italy). Continental Shelf Research 23, 1821–1831.

Wiener, J.G., Krabbenhoff, D.P., Heinz, G., Scheuhammer, A., 2003. Ecotoxicology of mercury. In: Hoffman, D.J., et al. (Eds.), Handbook of Ecotoxicology. Lewis, Boca Raton, FL, pp. 409–463.

Žagar, D., Knap, A., Warwick, J.J., Rajar, R., Horvat, M., Cetina, M., 2006. Modelling of mercury transport and transformation processes in the Idrijca and Soca River system. Science of the Total Environment 368, 149–163.

Žibret, G., Gosar, M., 2006. Calculation of the mercury accumulation in the Idrijca River alluvial plain sediments. Science of the Total Environment 368, 291–297.